Pamukkale Univ Muh Bilim Derg, 30(3), 395-404, 2024

Pamukkale Üniversitesi Mühendislik Bilimleri Dergisi

Pamukkale University Journal of Engineering Sciences

Efficiency of L-DOPA+TiO_2 modified RO membrane on salinity gradient energy generation by pressure retarded osmosis

L-DOPA+TiO_2 modifiye ters ozmoz membranının basınç gecikmeli osmoz ile tuzluluk gradyanı enerji üretimi üzerindeki verimliliği

Nuray ATES[1*], *Seda SAKİ*[2], *Murat GOKCEK*[3], *Nigmet UZAL*[4]

[1]Department of Environmental Engineering, Engineering Faculty, Erciyes University, Kayseri, Turkey.
nuraya@erciyes.edu.tr

[2]Department of Material Science and Mechanical Engineering, Engineering Faculty, Abdullah Gül University, Kayseri, Turkey.
seda_saki@hotmail.com

[3]Department of Mechanical Engineering, Engineering Faculty, Niğde Ömer Halisdemir University, Niğde, Turkey.
mgokcek@nigde.edu.tr

[4]Department of Civil Engineering, Engineering Faculty, Abdullah Gül University, Kayseri, Turkey.
nigmet.uzal@agu.edu.tr

Received/Geliş Tarihi: 17.03.2023 Revision/Düzeltme Tarihi: 03.07.2023 doi: 10.5505/pajes.2023.36690
Accepted/Kabul Tarihi: 21.07.2023 Research Article/Araştırma Makalesi

Abstract

Harvesting energy from the salinity gradient of seawater and river water using pressure retarded osmosis (PRO) has been a major research topic of recent years. However, there is a need for efficient PRO membranes that can generate high power density and are pressure resistant, as the performance of current membranes on the market is poor. In this study, specific energy potential of PRO process using L-DOPA+TiO_2 modified BW30-LE membrane was evaluated on synthetic and real water samples. Polyamide BW30-LE RO membrane was modified by L-DOPA, L-DOPA+0.5 wt% TiO_2 and L-DOPA+1 wt% TiO_2. The effect of hydraulic pressure and temperature on generation of power density were evaluated for 5, 10, and 15 bar pressures, as well as 10 °C, 20 °C, and 30 °C degrees. The incorporation of TiO_2 nanoparticles with L-DOPA increased the water flux by increasing the surface hydrophilicity and roughness of the membrane surface. The maximum specific power was observed as 1.6 W/m² for L-DOPA+1 wt% TiO_2 modified BW30-LE membrane at 15 bar pressure. Besides, Mediterranean and Aegean, Black Sea water samples were used as draw solution and Seyhan, Ceyhan, Buyuk Menderes, Gediz, Yesilirmak, and Kizilirmak Rivers were used as feed solution. The highest osmotic power density was obtained by using L-DOPA+1 wt% TiO_2 modified BW30-LE membrane with Ceyhan River as feed and Mediterranean Sea water as draw solution, which have the highest differences in salinity. In the mixture of Mediterranean and Ceyhan River, the highest power density was obtained at 10 bar pressure at 30 ± 5°C with 0.70 W/m².

Keywords: L-DOPA, Polyamide membrane, Pressure retarded osmosis, Salinity gradient power, Surface modification.

Öz

Basınç geciktirmeli osmoz (PRO) kullanarak deniz suyu ve nehir suyunun tuzluluk gradyanından enerji elde etmek son yıllarda önemli bir araştırma konusu olmuştur. Ancak, piyasadaki mevcut membranların performansı düşük olduğundan, yüksek güç yoğunluğu üretebilecek ve basınca dayanıklı etkili PRO membranlarına ihtiyaç duyulmaktadır. Bu çalışmada, sentetik ve gerçek su numuneleri kullanılarak L-DOPA+TiO_2 modifiye BW30-LE membranlar ile PRO prosesinin özgül enerji potansiyeli değerlendirilmiştir. Polyamid BW30-LE RO membranı, L-DOPA, L-DOPA+ %0.5 ağ. TiO_2 ve L-DOPA+ %1 ağ. TiO_2 ile modifiye edilmiştir. Hidrolik basınç ve sıcaklığın güç yoğunluğu üzerindeki etkisi 5, 10 ve 15 bar basınçları ile 10 °C, 20 °C ve 30 °C dereceleri için değerlendirilmiştir. TiO_2 nanoparçacıklarının L-DOPA ile birleştirilmesi, yüzey hidrofilikliğini ve membran yüzeyinin pürüzlülüğünü artırarak su akışını arttırmıştır. L-DOPA+ %1 ağ. TiO_2 ile modifiye edilmiş BW30-LE membran için 15 bar basınçta maksimum özgül güç 1,6 W/m² olarak gözlendi. Ayrıca, çekme çözeltisi olarak Akdeniz ve Ege, Karadeniz su örnekleri, besleme çözeltisi olarak Seyhan, Ceyhan, Büyük Menderes, Gediz, Yeşilırmak ve Kızılırmak nehirleri kullanılmıştır. En yüksek ozmotik güç yoğunluğu, L-DOPA+ %1 ağ. TiO_2 modifiye BW30-LE membranı ile tuzluluk farklılıkları en yüksek olan besleme çözeltisi olan Ceyhan Nehri ve çekme çözeltisi olan Akdeniz suyu kullanılarak elde edilmiştir. Akdeniz ve Ceyhan Nehri karışımında en yüksek güç yoğunluğu 10 bar basınçta 30 ± 5 °C'de 0,70 W/m² ile elde edilmiştir.

Anahtar kelimeler: L-DOPA, Poliamid membran, Basınç geciktirmeli osmoz, Tuzluluk gradyan enerjisi, Yüzey modifikasyonu.

1 Introduction

Salinity gradient energy refers to the renewable energy source to produce electricity generated by mixing entropy between two different salt concentration solutions [1]-[3]. Several technologies including reverse electrodialysis [4],[5] capacitive mixing [6] and pressure retarded osmosis (PRO) [1,][7] can be employed for harvesting of Gibbs free energy released as a result of salinity difference between sea and river waters [8]. PRO is known as a viable source for clean and renewable energy [9] due to some of its outstanding advantages, such as sustainable energy generation system, membrane-based compact system minimizing environmental impacts, and an extend range of applications where different water resources can be used [10],[11]. PRO uses a concentrated solution called the draw solution to create high osmotic pressure, which drives water across a semi-permeable membrane from the feed solution, which has low osmotic pressure. A hydraulic pressure lower than the difference in osmotic pressure is then applied to the draw solution to slow the osmotic permeation of water from the feed solution across the membrane, turning the osmotic energy into hydrostatic pressure in the expanded draw solution. The power density of the PRO membrane is linked to the power gained when the permeate goes through the energy

*Corresponding author/Yazışılan Yazar

recovery device and the pressure drops [12]. Salinity gradient-based energy generation is not only completely renewable and clean, but it also has negligible environmental impacts, with no significant emissions to the atmosphere (CO_2) or water bodies [11],[13]-[15]. The osmotic pressure difference between the feed and draw solutions with different salinities on both sides of the membrane causes pressurized water flow in the PRO system, and the hydroturbine generates electricity [9],[16]-[18]. With an achievable efficiency of 54–56 percent for the PRO process and power densities ranging from 2.3 to 38 W/m^2, previous studies have shown PRO as a potential source with greater efficiency and power density [8]. In theory, a stream flowing at 1 m^3/s when mixed with sea water of salinity 3.5% NaCl could produce 0.75-1 MW of electricity [19],[2],[20]. The approximate global osmotic energy production from the mixture of ocean and fresh river water in the estuaries is estimated 1750-2000 TWh/year [15],[21].

The PRO can be described as inverse procedure of reverse osmosis (RO), which is used to transfer the osmotic pressure of seawater from salt water to fresh water and initiate hydraulic pressure (i.e. energy) [1],[8]. Although there has been increased interest in salinity gradient-based energy generation in recent years, commercial RO membranes are not appropriate for PRO applications because of their hydrophobic, thick and low-porous support layer [1],[22]-[24]. The most crucial factor affecting efficiency of the PRO process works is power density. The permeability, selectivity, hydrophilicity and resistance to fouling of the membrane are factors that affect the power density [25],[8]. Moreover, commercial thin film composite (TFC) RO membranes can resist high hydraulic pressure but show relatively low power density in PRO studies because of severe internal concentration polarization [10],[26]-[28]. Therefore, it is necessary to develop and optimize semi-permeable PRO membranes for reasonable energy generation [18],[25],[29],[30].

Enhancing membrane hydrophilicity is a topic that is covered in a lot of research. The following four methods are typically used to improve the hydrophilicity of membranes: 1) incorporation of additives and/or co-solvent in the interfacial polymerization [31]-[33], 2) incorporation of nano-materials (carbon nanotubes, graphene oxide, zeolite, silica, titanium oxide etc.) into the membrane surface [34]-[38], 3) surface alteration of membrane by polymers or nanoparticles [39],[40], 4) submerging TFC membranes in certain solutions [33],[41]. L-DOPA (3- (3,4-Dihydroxyphenyl) -L-alanine), one of the functional monomers, has found widespread use to modify the membrane surface to provide membrane resistance against fouling [42]. L-DOPA, a zwitterionic substance having negative and positive charged groups, is regarded as a non-fouling substance and it can create more robust and stable electrostatic bonds with water than hydrophilic substances [42]. In the authors' previous work, as a result of modifying the surface of the RO membrane with L-DOPA, the membrane surface was altered to provide higher hydrophilicity and water permeability for advanced osmosis (FO) applications [43]. Additionally, it is a widespread procedure to incorporate nanoparticles onto membrane surfaces to enhance their hydrophilicity, permeability, and antifouling qualities. Nanomaterials have been applied to membrane surfaces to improve interfacial interactions between nanomaterials and the membrane active layer based on the unique adhesion property of L-DOPA [44].

The majority of the research in literature on PRO performance has used synthetic water samples in experimental studies. In real systems, the pretreated river water partially passes through the membrane module after going through the pretreatment process. Meanwhile, the seawater draw solution was initially employed pretreatment, then subjected to pressure exchange before entering the PRO membrane module. Thus, in comparison to synthetic feed and draw water samples, sea and river waters have complex background water qualities. The energy potential of the PRO process using a modified RO membrane was evaluated on synthetic and real water samples in this study. In the scope of the study, 1) BW30-LE RO membrane was modified using L-DOPA+TiO_2 and 2) energy efficiencies using Mediterranean, Aegean and Black Sea as a draw solution and Seyhan, Ceyhan, Kizilirmak, Buyuk Menderes, Gediz Rivers as feed solution were investigated by PRO technology. The PRO osmotic power potential was investigated by lab-scale experiments using L-DOPA+TiO_2 modified commercial RO BW30-LE membrane. In terms of membrane performance, draw solution concentration, hydraulic pressure differences, and temperature, the practical implications of real river water and seawater samples were evaluated. As far as we can tell, no experimental data for Turkey's power density and energy efficiency potential have been presented. Moreover, more than 20 countries, including Turkey, border the Mediterranean, Aegean, and Black Seas. The findings of this study also provide crucial information for these countries' energy output based on salinity differences. Therefore, this study is significant for the existing literature that supports the use of PRO membrane technology.

2 Materials and methods

2.1 Membrane and chemicals

In this study, flat-sheet polyamide BW30-LE RO membrane was tested (DOW, USA). For membrane modification, 3-(3,4-Dihydroxyphenyl)-L-alanine (L-DOPA) and Tris (hydroxymethyl) aminomethane from Sigma Aldrich, isopropyl alcohol and sodium chloride (NaCl) from Merck were purchased. Titanium dioxide (TiO_2) nanoparticle (99%, anatase) with particle size of 10-25 nm was purchased from Nanografi, Turkey. Pure water experiments were conducted using deionized (DI) water produced by Millipore Direct Q8-UV.

2.2 BW30-LE RO membrane surface modification

BW30-LE was soaked in distilled and deionized (DDI) water for 12 hours at ambient temperature (20 ± 5 °C) to wet out the membrane pores before modification with L-DOPA + TiO_2. The buffer solution of Tris–aminomethane (10 mM, pH 8.3) was used to dissolve L-DOPA (2g/L) and mixed during 12 h. Then, 0.5 wt%, 1wt% TiO_2 nanoparticles were added L-DOPA solution and stirred for 24 h. The surface coating was performed at ambient temperature (20 ± 5 °C) by a crossflow membrane filtration system. The surface of membrane (150 cm^2 area) was coated with L-DOPA and L-DOPA+TiO_2 solutions facing the active sites of membranes surfaces for 6 hours in total recycling mode. After that, the coated membranes were rinsed 3 times for 1.5 h with DDI water to eliminate the residual chemicals from the surface of the membrane. The modified membranes were then soaked in isopropyl alcohol solution (25% v/v) for 15 min to clean the residuals. The membranes modified and used in experiments were kept in refrigerator at +4°C [43].

2.3 Characterization of membranes

2.3.1 Scanning electron microscope (SEM) images

The surface morphologies of BW30-LE RO membranes modified with L-DOPA and L-DOPA+TiO_2 were observed with SEM instrument of Zeiss Leo 440 at 10KV. All samples were dried for 12 hours at 80 °C in oven before scanning membrane morphologies.

2.3.2 Atomic force microscopy (AFM)

MultiMode 8-HR, VEECO model AFM instrument was used for characterization of virgin and modified membranes. The surface topologies and average surface roughness (Ra) of the selective layer of the membranes were identified by root mean square roughness (Rq) and the maximum height of the membrane profile (Rmax). AFM instrument equipped with trapping mode (Model: RTESP-300) with a scan size of 5 µm × 5 µm was run in the contact mode. Before taking AFM images, the membranes were held in oven during overnight at 80°C to dry.

2.3.3 Filtration experiments

Separation properties of membranes with respect to pure water (DDI) permeability (A), salt permeability (B) and salt rejection (R) were defined by conductivity measurements for both the feed solution (2 g/L NaCl) and permeates at 15 bar pressure in a crossflow membrane cell (Sterlitech, HP4750, USA). Mesh spacers were used in membrane cell for preventing concentration polarization. The permeate flux was monitored at a trans-membrane pressure of 15 bar (ΔP) during certain period (Equation 1):

$$J_W = \frac{\Delta V}{A_s * \Delta t} \quad (1)$$

Where, J_W is the permeate flux (L/m²h), V is volume of water passed through membrane (L), A_s is the effective surface area of membrane (m²), and t is the filtration period (h).

The distilled water permeability (A), salt permeability (B) and salt rejection (R) were computed according to the Equations 2-4:

$$A = \frac{Jw}{\Delta P} \quad (2)$$

$$R = \left(1 - \frac{Cp}{Cf}\right) * 100 \quad (3)$$

$$B = \frac{A(1-R)(\Delta P - \Delta\pi)}{R} \quad (4)$$

Here, Cf and C_p are the feed and permeate salt concentrations, Δπ denotes osmotic pressure.

The osmotic pressure Δπ was calculated using Equation 5 given below. The i is Van't Hoff constant, C represents the amount of dissolved ions (moles) in the solution, T is temperature in K unit, R is universal gas constant (0.083145 L.bar/moles.K), and φ is osmotic pressure constant.

$$\Delta\pi = i.\varphi.C.R.T \quad (5)$$

2.3.4 FO experiments

For the preliminary evaluation of the PRO performances of L-DOPA and L-DOPA+ (0.5% and 1%) TiO_2 modified BW30-LE membranes, laboratory-scale process experiments were carried out in FO mode. A bench-scale FO module was conducted using a membrane with an active area of 48 cm² in experiments. In the FO system, the feed and draw solutions were operated under countercurrent crossflow, which was recirculated in a closed system. The temperatures of feed and draw solution were adjusted at 20±5 °C. The draw solutions concentrations were prepared as 35 and 50 g/L to simulate and compare the salinity degree of the sea waters. Feed (DDI water) and draw solutions (NaCl: 35 and 50 g/L) were recirculated at a flow rate of 1.64 and 2.45 mm/s, respectively using two peristaltic pumps (Masterflex, model 77201-62). The flux was monitored by recording change in mass of the draw solution with a digital balance providing data transfer to the computer. The active layer of membrane was oriented in PRO mode. The change in mass, conductivity, pH and temperature values in the draw solution were monitored every 15 minutes for 2 hours.

2.4 PRO experiments

Synthetic and real water samples were used to examine the power production potential of L-DOPA+TiO_2 modified BW30-LE membrane. Modified membrane (150 cm² an active area) was placed in a bench-scale PRO module connected by a digital balance, two containers for feed and draw solutions, peristaltic pumps and multimeter for temperature, pH and conductivity measure. In PRO experiments, 2 M NaCl as draw solution and DDI water as feed solution were used. The feed solution was fed with DDI water to prevent the reverse salt flux during the experiments. Various pressures (5, 10 and 15 bar) were employed to draw face to determine the hydraulic pressure effect. The effect of temperature on power production potential for synthetic water using BW30-LE membrane was also evaluated for three different temperatures as 10, 20 and 30±5⁰C at pressures of 5, 10 and 15 bar. Feed and permeate samples were collected every 15 minutes for 2 hours during the filtration operation to monitor flux development.

For the PRO experiments using real waters were sampled from the mixing points of Seyhan, Ceyhan, Kizilirmak, Yesilirmak, Buyuk Menderes and Gediz and rivers which poured into the seas from the Mediterranean, Aegean, and Black Sea. A total of 50 L water samples from each sampling point were taken into 5 L PVC jerricans and kept in isolated containers with ice molds until the samples reached to the laboratory. Prior to PRO experiments real water samples were filtered through the 45 µm cartridge filter to remove impurities for preventing membrane fouling. Water flow, pH, conductivity, pressure and temperature values were followed in all PRO tests and weight increments of draw solution was logged at each quarter hour by a digital balance at a constant temperature (20±5 °C) during the experiments. The flux was computed according to Equation 1. ΔP.

The power density was determined according to Equation 6:

$$W = J_W * \Delta P \quad (6)$$

Where, W: power output per square meter of membrane (W/m²) and it can be determined by multiplication of water flux (Jw, L/m²h) with hydraulic pressure (ΔP, bar).

The temperature change caused by heat transfer across the membrane has a significant impact on water flow in PRO [45]. The impact of temperature on PRO efficiency were evaluated by applying varied temperatures from 10±5 °C to 30±5 °C to represent the different conditions of seawater. All PRO experiments were replicated.

2.5 Description of the rivers

The salinity gradient based energy production was evaluated by PRO process using real water samples collected from Ceyhan, Seyhan, Buyuk Menderes, Gediz, Kizilirmak and Yesilirmak Rivers and Mediterranean, Eagen and Black Sea. Selected rivers and seas are shown in Figure 1. Turkey's longest river Kizilirmak River with 1,355 km length flows into the Black Sea river born in Eastern Anatolia. The average flowrate of Kizilirmak is 58 m^3/s. Yesilirmak River has 519 km length with average flowrate 145 m^3/s and it borns in Northeast Anatolia and flows into the Black Sea. Büyük Menderes, the largest river in Western Anatolia, is the main irrigation source of the basin. The river, which is 548 km long, flows into the Aegean Sea and its average flow is 34 m^3/s. The Gediz River is the second largest river after the Buyuk Menderes River, which flows into the Aegean Sea. Its length up to the point where it reaches the sea in the Aegean is 401 km and average flowrate is 23 m^3/s. The Ceyhan River in the Mediterranean region is 509 km long and is one of the longest rivers. The flow rate of the river, which is 149 m^3/s on average, increases to 380 m^3/s temporarily with the effect of autumn rains. The Seyhan River which originates in the Middle East Anatolia and flows into the Mediterranean Sea is one of the major rivers in Mediterranean Region with average flow of 103 m^3/s and length of 850 km.

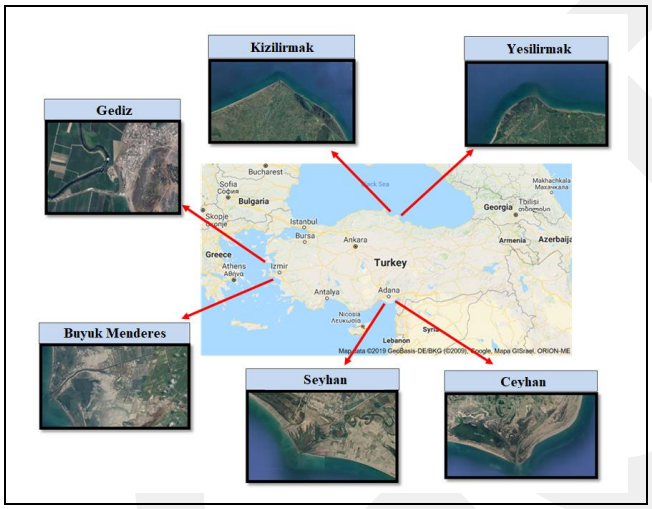

Figure 1. Aerial view of selected estuaries in Turkey: Ceyhan, Seyhan, Buyuk Menderes, Gediz, Kizilirmak and Yesilirmak Rivers.

3 Results and discussions

3.1 Characterization of membranes

3.1.1 SEM images

The SEM images of the L-DOPA and L-DOPA+TiO_2 modified BW30-LE RO membranes were shown in Figure 2. It is clearly shown that some new regular nodules appeared on L-DOPA+1 wt% TiO_2 modified membranes compared to L-DOPA modified membrane. The formation of these new nodules was attributed probably due to the connection of the L-DOPA and TiO_2 nanomaterials on the membrane surface. Besides, TiO_2 nanoparticles were completely coated on the membrane surface by polydopamine (PDA), which also provided a uniform structure. Modification of the membranes enabled it to form strong coordination bonds between the membranes and nanoparticles when catechol/quinone groups within the structure of polydopamine (PDA) come into contact with a TiO_2 suspension [46]-[49]. Shabani et al. [50] stated that the putting of dopamine to the PVC surface changed both the surface and cross-section morphologies by creating longer and wider leaves on the surface, resulting in increased water permeability.

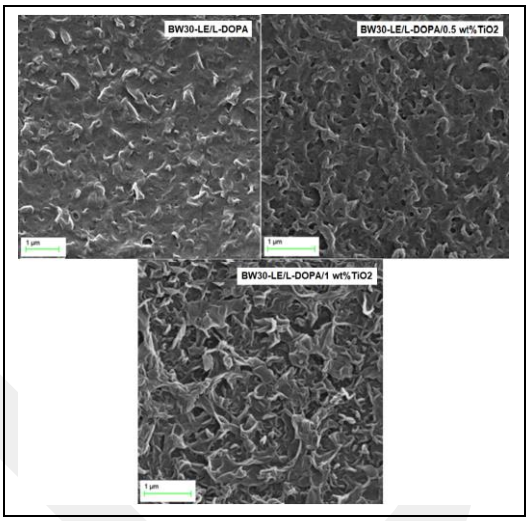

Figure 2. SEM images of L-DOPA and L-DOPA+TiO_2 modified BW30-LE RO membranes.

3.1.2 AFM analysis

In Figure 3, three-dimensional 5 µm scans AFM images of L-DOPA and L-DOPA+TiO_2 modified BW30-LE RO membranes were given. The L-DOPA modified membrane demonstrated a uniform and nodular structure as it's revealed in figure.

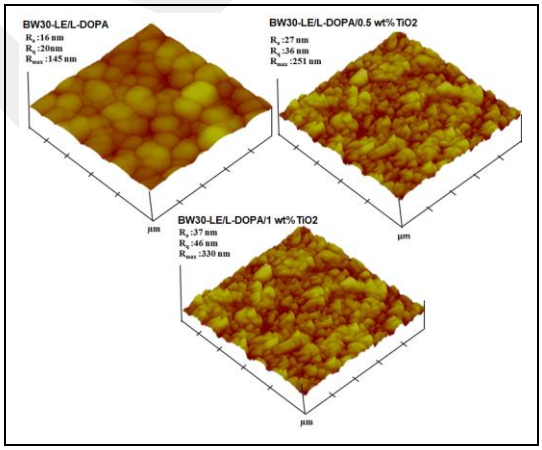

Figure 3. AFM images of L-DOPA and L-DOPA+TiO_2 modified BW30-LE RO membranes.

Through coating by L-DOPA + TiO_2, all membrane surfaces were covered by new nodules with distinctive ridge and valley structure. The morphological analyses of SEM and AFM images affirmed that the TiO_2 nanoparticle were effectively attached onto the surface of BW30-LE RO membrane. Following modification with L-DOPA and L-DOPA + TiO_2, respectively, the results demonstrated an increase in the average surface roughness of the membrane from 16 nm to 27 nm and 37 nm, respectively. According to the outcomes of a study by Van Wagner et al. [51], employing poly(ethylene glycol) diglycidyl ether to modify RO membrane surfaces led to an increase in roughness of 19–33%. Similarly, the roughness of the membrane was increased from 104.20 nm to 310.25 nm when polyamide membrane incorporated with 0.3 wt% TiO_2 [52].

Shabani et al. [50] observed that the surfaces of dopamine-modified PVC membranes became rougher, and moreover, the roughness increased with the increase of dopamine amount.

3.1.3 Filtration experiments

For virgin, L-DOPA and L-DOPA+TiO_2 modified BW30-LE RO membranes, the NaCl salt rejection and the permeability coefficients of water and salt were summarized in Table 1.

Table 1. Water and NaCl salt permeabilities and NaCl salt rejections for the virgin and modified BW30-LE RO membranes.

Membrane	A (L/m²h.bar)	B (L/m²h)	R (%)
BW30-LE	2.80	0.69	98.2
BW30-LE/L-DOPA	3.40	0.84	98.2
BW30-LE/L-DOPA/0.5 wt%TiO_2	3.69	1.12	97.8
BW30-LE /L-DOPA/1 wt%TiO_2	3.98	1.21	97.8

The flux of the modified membranes increased by 33% and 44%, respectively, in consequence of coating with and L-DOPA +0.5% wt TiO_2 and L-DOPA +1% wt TiO_2. The water permeability enhanced from 3.69 to 3.98 L/m²h.bar as increasing concentration of TiO_2 from 0.5 to 1% wt at operating pressure of 15 bar. The previous studies reported that the incorporation of TiO_2 nanoparticles in PA layer was enhanced the surface hydrophilicity [34],[53]. The increased water permeability of the TFC RO membrane is primarily due to the high diffusion rate of water molecules caused by the increased membrane hydrophilicity. Furthermore, the increase in water flow can be caused by TiO_2 nanoparticles added to the membrane structure, which affects the interfacial polymerization process and changes the crosslinking condition. Likewise, increased roughness on the membrane surface can contribute to flux development by increasing the surface area available to transport water through the membrane pores [36],[54]-[56]. Besides, improvement of permeability and extension of fouling by modification of membrane lead to longer the lifespan of the membrane and facilitate practical industrial applications [57]. In the study of Li et al. [58], polyamide TFC RO membrane was modified with carbon dots and enhanced water flux as a result of increased roughness was attributed the formation of leaf-like structure into ridge-and-valley structure. Similarly, Azad et al. [59] stated improvement of the water permeation by loading of hydrophilic TiO_2 nanoparticles to the membranes and they observed about 14% and 15% of water flux increase in the PRO and FO systems by incorporation of 1 wt% TiO_2 to the membrane matrix, respectively.

Regarding salt rejection, L-DOPA and L-DOPA+TiO_2 modified BW30-LE RO membranes exhibited over 97% of NaCl rejection when tested with 2 g/L NaCl feed solution at 15 bar. El-Aassar [53] reported an improvement in water flux and salt rejection of TiO_2 modified PA membrane. L-DOPA+TiO_2 modified membranes (0.5wt% and 1wt%) compared to L-DOPA modified membrane demonstrated similar salt rejections with 98.2% and 97.8%, respectively. Nevertheless, the relative deterioration of salt rejection for nanoparticle added membranes has been attributed to lesser degree of cross-linking and expanding micro-voids between nanofillers and polymer matrix [37]. Based on these results, the L-DOPA+1 wt% TiO_2 modified BW30-LE membrane seems better for FO application owing to its high-water permeability, comparable salt rejection, and B/A ratio [60].

3.1.4 FO experiments

In order to assess the water flux change for virgin and L-DOPA+TiO_2 modified membranes, FO system was operated using a DDI water as a feed solution and 35 and 50 g/L NaCl solutions as the draw solution. The water fluxes of L-DOPA and L-DOPA+TiO_2 modified BW30-LE membranes in FO process were summarized in Table 2. The FO water flux increased from 4.3 to 14.1 L/m²h in the 35 g/L NaCl solutions and 4.8 to 14.2 L/m²h in the 50 g/L NaCl solutions as the concentration of TiO_2 nanoparticle increased from 0.5 to 1% wt. The inclusion of TiO_2 nanoparticles into the membrane structure can enhance the permeability of the TFC membrane and consequently resulted as an increase in FO flux [61]. Therefore, it has been confirmed that the approach of modifying BW30-LE membrane surface properties by incorporation of L-DOPA + TiO_2 could be effective to improve FO performance.

Table 2. FO flux of the virgin and modified BW30-LE RO membranes at different draw solution concentrations (35g/L and 50 g/L).

	BW30-LE		BW30-LE/ L-DOPA		BW30-LE/ L-DOPA +% 0.5 TiO_2		BW30-LE/ L-DOPA +% 1 TiO_2	
NaCl (g/L)	35	50	35	50	35	50	35	50
Flux (L/m²h)	0.4	0.8	2.6	3.5	4.3	4.8	14.1	14.2

3.2 Power production from salinity gradient: PRO Tests

3.2.1 Power production of synthetic water experiments

The effect of hydraulic pressure on the power generation performance of BW30-LE membranes modified with L-DOPA and L-DOPA+TiO_2 using DDI water as feed and 2M NaCl solutions as draw solutions were assessed at 5, 10 and 15 bars pressure at constant temperature of 20±5°. The power density generations of the modified membranes as a function of hydraulic pressure were illustrated in Figure 4.

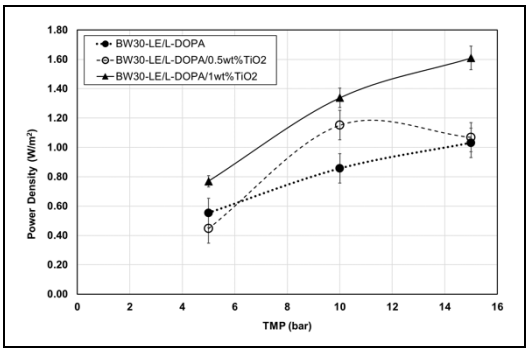

Figure 4. Power density of L-DOPA and L-DOPA+TiO_2 modified BW30-LE membrane at different transmembrane pressures.

As seen from the figure, the maximum specific power was observed as 1.6 W/m² for L-DOPA+1 wt% TiO_2 modified BW30-LE membrane at 15 bar pressure with 2 M draw solution salt concentration. Although power density improved by increasing hydraulic pressure for L-DOPA and L-DOPA+1 wt% TiO_2 modified membranes, it was decreased in L-DOPA+0.5 wt%

TiO_2 modified membrane at 15 bar. Madsen et al. [62] observed around 1.75 W/m² energy production by mixing geothermal water (feed) and 310 mg/L salt water at 60 bar pressure. They implied that salt water has significant impact on energy production and increasing salt water from 30 g/L to 310 g/L increase the energy production from 0.1 to 1.75 W/m² at 60 bar pressure [63]. Kim and Elimelech [64] observed water flux of 13.9 L/m²h and power density of 4.7 W/m² when 12.5 bar hydraulic pressure was applied with 0.5 M (feed) and 2 M (draw) NaCl solutions using a commercial FO membrane. On the other hand, a maximum power density of 0.73 W/m² was observed at a hydraulic pressure difference of about 10 bar using 1 M draw and 0.5 M feed solutions. Lin et al. [65] reported the power densities of under 2 W/m² using river water with 0.015 M NaCl and sea water with 0.6 M NaCl in countercurrent operation.

3.2.2 Effect of temperature on power production

Figure 5 demonstrates the effect of temperature on PRO performance using L-DOPA+1 wt% TiO_2 modified BW30-LE membrane. The temperature effect on modified membrane was evaluated at different pressures of 5, 10 and 15 bar. Obviously PRO performance has been significantly improved due to temperature increase, especially from 10°C to 20°C and 30°C degrees. The power density advanced from 0.41 to 0.78 W/m², almost doubling as the temperature increased from 10°C to 20°C and 30°C at 5 bar pressure, respectively. The lowest power densities were observed at temperature of 10°C ±5°C that was 0.41 W/m², 0.67 W/m² and 0.47 W/m² for 5, 10 and 15 bar pressures, respectively. Although an increase in the temperature from 20°C to 30°C had no effect on the power density at 5 and 10 bar pressures, the power density increased by about 12% from 1.6 to 1.76 W/m² with the temperature increase for 15 bar pressure. Meanwhile, an increase was observed in the water flux as the temperature increased in the PRO processes. The flux was increased from 1.12 to 3.83 and 4.19 L/m²h, almost three to four times as the temperature increased from 10°C to 20°C and 30°C at 15 bar pressure, respectively. Increments in temperature causes changes in the hydrodynamic conditions (osmotic pressure, viscosity, density, and diffusivity) of feed and draw solutions, which directly affects the membrane performance [66],[67]. Thus, increasing solution temperatures is anticipated to potentially enhance the anticipated power density [68]. According to Adhikary et al. [67] the power density increased by roughly 34% by raising temperature from 20 °C to 40 °C. Abdelkader and Sharqawy [69] reported about 130% power density increase by raising the temperature of the solutions from 20 °C to 50 °C increases.

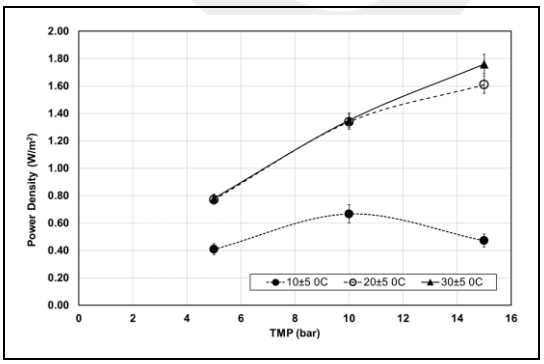

Figure 5. Power density of L-DOPA+1wt% TiO_2 modified BW30-LE membrane at different temperatures.

3.2.3 Power production of real-water experiments

Monthly salinity values of Turkish Rivers showed much greater variability. According to long-term data, average annual salinity values vary with time and climate changes. The selected rivers of Seyhan and Ceyhan, Kizilirmak and Yesilirmak, Buyuk Menderes and Gediz are flowing into the Mediterranean, Black and Aegean Sea, respectively. The conductivity values of rivers and seas were monitored during PRO experiments and given in Table 3.

Table 3. Conductivity values of tested rivers and seas in PRO experiments.

Conductivity of Rivers (µS/cm)					
Ceyhan	Seyhan	Kizilirmak	Yesilirmak	Gediz	B.Menderes
450-540	580-700	1,730-1,750	500-530	610-750	1,960-2,000

Conductivity of Seas (µS/cm)		
Mediterranean	Black	Aegean
55,000-60,000	24,000-26,000	46,000-50,000

These rivers are described for their low salinity, varying between 0.1% and 0.5%. While the lowest conductivity was observed for Ceyhan River ranging from 450 to 540 µS/cm, the highest conductivity was monitored for Buyuk Menderes varied between 1,960 and 2,000 µS/cm. Among all tested sea water samples, the highest conductivity was observed for Mediterranean Sea in the range of 55,000 and 60,000 µS/cm. In previous studies, the average salinity of Black Sea [70], Mediterranean [71] and Aegean [72] seawaters were reported with 18%, 36% and 35%, respectively. Similarly, our experimental results showed that the Mediterranean has the highest and Black Sea has the lowest conductivity value (Table 3).

L-DOPA+1wt% TiO_2 modified BW30-LE membrane which showed the highest filtration performance and salinity rejection in previous experiments was tested using real water sources collected from the mixing points of selected rives and seas to examine the power density. In Figure 6, power density variation based on pressure difference across BW30-LE membrane modified with L-DOPA+1% by weight TiO_2 is presented.

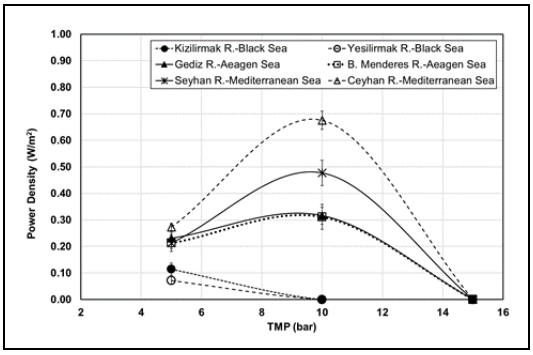

Figure 6. Power density of L-DOPA+1wt% TiO_2 modified BW30-LE membrane versus pressure for selected river-sea couples.

Between these rivers and seas, the river-sea couple with the highest differences in salinity (Seyhan River-Mediterranean Sea) provided higher osmotic energy production. Depending on

the energy production experiments, the highest osmotic power was obtained between Ceyhan River and the Mediterranean, with the highest difference in conductivity. Although the salinity of the rivers (B.Menderes-Gediz or Kizilirmak-Yesilirmak) flowing into the same sea (Aegean or Black Sea) is about 3 times different from each other, the energy production efficiency is almost the same.

In order to determine the temperature and pressure effects on energy production in salinity gradient system, Mediterranean Sea and Ceyhan River samples were tested using L-DOPA/1wt%TiO_2 modified BW30-LE membrane. Experimental studies were conducted at three different temperatures of 10±5 °C, 20±5 °C and 30±5 °C for 5, 10 and 15 bar pressures. As shown from Figure 7, power density is getting higher as increasing temperature. Although the highest power density was observed at 30±5 °C for 10 bar pressure, the power density values for temperatures of 20 and 30 °C were very close to each other, power density increased by 1.2% for each degree of temperature increase. Since the reported average water temperature of Mediterranean Sea in 2021 was 22.2 °C [73], the results of our experiments indicated that practical energy optimization could be achieved for the Mediterranean Sea and Seyhan River couple.

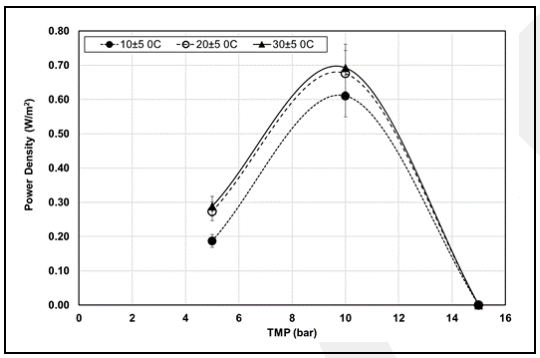

Figure 7. Power density of L-DOPA+1wt% TiO_2 modified BW30-LE membrane mixing point of Mediterranean Sea and Ceyhan River at different temperatures.

The highest power density values for all temperatures were observed at 10 bar pressure. The power densities increased by almost three times when pressure doubled. However, no flux was obtained for 15 bar pressure; hence no power density could be calculated. The increase in temperature affects the intrinsic characteristics of membrane system and increases the water and salt flow. As a result, power density is expected to increase at higher temperatures due to increased water flow [15],[20],[74]. Touati et al. [74] and Touati et al. [75] reported that power density increased by 1% for each degree of temperature increase. As the temperature increased from 20 °C to 60 °C, the power density increased by 0.33 W/m² for the cellulose triacetate membrane. Kim and Elimelech [64] observed an increase in water flux of 7.1%, 3.9%, and 5.0% for each degree of temperature increase, respectively, in their study performed at 20 °C and 30 °C temperature using 0.5 M NaCl feed solution against 1 M, 1.5 M, and 2 M NaCl draw solution. She et al. [76] stated that the increase in temperature affected water and salt permeability, and once the temperature was elevated from 25 °C to 35 °C, the specific power increases by 3.4% for each degree temperature. The improvement in water flux was attributed to increased diffusivity as temperature increased and decreased concentration polarization in the membrane support.

4 Conclusions

In this research, polyamide BW30-LE RO membrane was modified by L-DOPA, L-DOPA+0.5 wt% TiO_2 and L-DOPA+1 wt% TiO_2 and characterized by SEM and AFM image with respect to surface morphology, topology, roughness. Incorporation of TiO_2 to L-DOPA for modification of membrane improved modification of membrane that new regular nodules appeared on L-DOPA+1 wt% TiO_2 modified membranes compared to L-DOPA modified membrane. Morphological analysis including SEM and AFM images confirmed that TiO_2 nanoparticles successfully adhered to the structure of a commercial RO membrane.

Filtration experiments performed on FO process revealed that the fluxes of the L-DOPA+TiO_2 modified membranes increased by 33% and 44%, respectively, as a result of coating with L-DOPA+ 0.5% and 1% TiO_2. According to the filtration results, modification of the BW30-LE membrane with L-DOPA + 1 wt% TiO_2 appears to be better for FO application in terms of high-water permeability, rejection.

The maximum specific power generation was observed as 1.76 W/m² for L-DOPA+1 wt% TiO_2 modified BW30-LE membrane at 15 bar pressure with 2 M NaCl and distilled water couple as draw and feed solutions. Power density was improved by 12% as increasing temperature from 20 °C to 30 °C at 15 bar pressure.

Furthermore, the efficiencies of modified RO membranes by L-DOPA + TiO_2 was assessed regarding with permeate flux and power density using real river water (Ceyhan, Seyhan, Buyuk Menderes, Gediz, Kizilirmak, and River) and sea water (Mediterranean, Aegean, and Black Sea) samples collected from mixing points in Turkey. The Ceyhan River-Mediterranean Sea couple system with L-DOPA+1wt % TiO_2 modified BW30-LE membrane demonstrated the highest power density of 0.70 W/m² at 10 bar pressure and 30 °C temperature.

5 Acknowledgements

The authors gratefully acknowledge the Scientific and Technological Research Council of Turkey for financial support (Project No. 115Y617).

6 Authors contribution statements

Nuray ATES, Designing the work, data analysis, formal editing, visualization, writing the manuscript, review and editing. Seda SAKI: Experimental study, data analysis, writing the manuscript. Murat GOKCEK, Designing the work, data analysis, review. Nigmet UZAL, Designing the work, data analysis, formal editing, visualization, writing the manuscript, review and editing. All authors read and approved the final manuscript.

7 Ethics committee approval and conflict of interest statement

"There is no need to obtain permission from the ethics committee for the article prepared".

"There is no conflict of interest with any person/institution in the article prepared".

8 References

[1] Achilli A, Childress AE. "Pressure retarded osmosis: From the vision of sidney loeb to the first prototype installation-Review". *Desalination*, 261(3), 205-211, 2010.

[2] Logan BE, Elimelech M. "Membrane-based processes for sustainable power generation using water". *Nature*, 488(7411), 313-319, 2012.
[3] Islam MS, Sultana S, Adhikary S, Rahaman MS. "Highly effective organic draw solutions for renewable power generation by closed-loop pressure retarded osmosis". *Energy Conversion and Management*, 171, 1226-1236, 2018.
[4] Post JW, Hamelers HVM, Buisman CJN. "Energy recovery from controlled mixing salt and fresh water with a reverse electrodialysis system". *Environmental Science & Technology*, 42(15), 5785-5790, 2008.
[5] Dlugolecki P, Gambier A, Nijmeijer K, Wessling M. "Practical potential of reverse electrodialysis as process for sustainable energy generation". *Environmental Science & Technology*, 43(17), 6888-6894, 2009.
[6] Brogioli D. "Extracting renewable energy from a salinity difference using a capacitor". *Physical Review Letters*, 103(5), 1-4, 2009.
[7] Loeb S, Norman RS. "Osmotic Power Plants". Science, 189(4203), 654-655, 1975.
[8] Sharma M, Das PP, Chakraborty A, Purkait MK. "Clean energy from salinity gradients using pressure retarded osmosis and reverse electrodialysis: A review". *Sustainable Energy Technologies and Assessments*, 49, 1-13, 2022.
[9] Achilli A, Cath TY, Childress AE. "Power generation with pressure retarded osmosis: An experimental and theoretical investigation". *Journal of Membrane Science*, 343(1-2), 42-52, 2009.
[10] Moon SJ, Lee SM, Kim JH, Park SH, Wang HH, Kim JH, Lee YM. "A highly robust and water permeable thin film composite membranes for pressure retarded osmosis generating 26 w.M(-2) at 21 bar". *Desalination*, 483, 1-10, 2020.
[11] Zoungrana A, Cakmakci M. "From non-renewable energy to renewable by harvesting salinity gradient power by reverse electrodialysis: A review". *International Journal of Energy Research*, 45(3), 3495-3522, 2021.
[12] Lee J, Kim S. "Predicting power density of pressure retarded osmosis (PRO) membranes using a new characterization method based on a single pro test". *Desalination*, 389, 224-234, 2016.
[13] Jones AT, Finley W. "Recent developments in salinity gradient power*". Oceans 2003 Mts/IEEE: Celebrating the Past-Teaming toward the Future*, 2284-2287, 2003.
[14] Gerstandt K, Peinemann KV, Skilhagen SE, Thorsen T, Holt T. "Membrane processes in energy supply for an osmotic power plant". *Desalination*, 224(1-3), 64-70, 2008.
[15] Thorsen T, Holt T. "The potential for power production from salinity gradients by pressure retarded osmosis". Journal of Membrane Science, 335(1-2), 103-110, 2009.
[16] Straub AP, Yip NY, Elimelech M. "Raising the bar: Increased hydraulic pressure allows unprecedented high power densities in pressure-retarded osmosis". *Environmental Science & Technology Letters*, 1(1), 55-59, 2014.
[17] Li MH. "Systematic analysis and optimization of power generation in pressure retarded osmosis: Effect of multistage design". *AICHE Journal*, 64(1), 144-152, 2018.
[18] Gonzales RR, Abdel-Wahab A, Adham S, Han DS, Phuntsho S, Suwaileh W, Hilal N, Shon HK. "Salinity gradient energy generation by pressure retarded osmosis: A review". *Desalination*, 500, 1-27, 2021.
[19] Wick GL, Schmitt WR. "Prospects for renewable energy from sea". *Marine Technology Society Journal*, 11(5-6), 16-21, 1977.
[20] Yip NY, Elimelech M. "Thermodynamic and energy efficiency analysis of power generation from natural salinity gradients by pressure retarded osmosis". *Environmental Science & Technology*, 46(9), 5230-5239, 2012.
[21] Wei J, Li Y, Setiawan L, Wang R. "Influence of macromolecular additive on reinforced flat-sheet thin film composite pressure-retarded osmosis membranes". *Journal of Membrane Science*, 511, 54-64, 2016.
[22] Lee KL, Baker RW, Lonsdale HK. "Membranes for power-generation by pressure-retarded osmosis". *Journal of Membrane Science*, 8(2), 141-171, 1981.
[23] Cath TY, Childress AE, Elimelech M. "Forward osmosis: Principles, applications, and recent developments". *Journal of Membrane Science*, 281(1-2), 70-87, 2006.
[24] McCutcheon JR, Elimelech M. "Influence of membrane support layer hydrophobicity on water flux in osmotically driven membrane processes". *Journal of Membrane Science*, 318(1-2), 458-466, 2008.
[25] Hickenbottom KL, Vanneste J, Elimelech M, Cath TY. "Assessing the current state of commercially available membranes and spacers for energy production with pressure retarded osmosis". *Desalination*, 389, 108-118, 2016.
[26] Mehta GD, Loeb S. "Internal polarization in the porous substructure of a semipermeable membrane under pressure-retarded osmosis". *Journal of Membrane Science*, 4(2), 261-265, 1978.
[27] Kuang W, Liu ZN, Yu HJ, Kang GD, Jie XM, Jin Y, Cao YM. "Investigation of internal concentration polarization reduction in forward osmosis membrane using nano-caco3 particles as sacrificial component". *Journal of Membrane Science*, 497, 485-493, 2016.
[28] Boruah PK, Sharma B, Hussain N, Das MR. "Magnetically recoverable Fe_3O_4/graphene nanocomposite towards efficient removal of triazine pesticides from aqueous solution: Investigation of the adsorption phenomenon and specific ion effect". *Chemosphere*, 168, 1058-1067, 2017.
[29] Lim S, Park MJ, Phuntsho S, Mai-Prochnow A, Murphy AB, Seo D, Shon H. "Dual-layered nanocomposite membrane incorporating graphene oxide and halloysite nanotube for high osmotic power density and fouling resistance". *Journal of Membrane Science*, 564, 382-393, 2018.
[30] Gonzales RR, Park MJ, Bae TH, Yang YQ, Abdel-Wahab A, Phuntsho S, Shon HK. "Melamine-based covalent organic framework-incorporated thin film nanocomposite membrane for enhanced osmotic power generation". *Desalination*, 459, 10-19, 2019.
[31] Jegal J, Min SG, Lee KH. "Factors affecting the interfacial polymerization of polyamide active layers for the formation of polyamide composite membranes". *Journal of Applied Polymer Science*, 86(11), 2781-2787, 2002.
[32] Ghosh AK, Jeong BH, Huang XF, Hoek EMV. "Impacts of reaction and curing conditions on polyamide composite reverse osmosis membrane properties". *Journal of Membrane Science*, 311(1-2), 34-45, 2008.
[33] Cui Y, Liu XY, Chung TS. "Enhanced osmotic energy generation from salinity gradients by modifying thin film composite membranes". *Chemical Engineering Journal*, 242, 195-203, 2014.

[34] Lee HS, Im SJ, Kim JH, Kim HJ, Kim JP, Min BR. "Polyamide thin-film nanofiltration membranes containing TiO_2 nanoparticles". *Desalination*, 219(1-3), 48-56, 2008.
[35] Ma N, Wei J, Liao RH, Tang CYY. "Zeolite-polyamide thin film nanocomposite membranes: Towards enhanced performance for forward osmosis". *Journal of Membrane Science*, 405, 149-157, 2012.
[36] Niksefat N, Jahanshahi M, Rahimpour A. "The effect of SiO_2 nanoparticles on morphology and performance of thin film composite membranes for forward osmosis application". *Desalination*, 343, 140-146, 2014.
[37] Zhao HY, Qiu S, Wu LG, Zhang L, Chen HL, Gao CJ. "Improving the performance of polyamide reverse osmosis membrane by incorporation of modified multi-walled carbon nanotubes". *Journal of Membrane Science*, 450, 249-256, 2014.
[38] Shen L, Xiong S, Wang Y. "Graphene oxide incorporated thin-film composite membranes for forward osmosis applications". *Chemical Engineering Science*, 143, 194-205, 2016.
[39] Vatanpour V, Zoqi N. "Surface modification of commercial seawater reverse osmosis membranes by grafting of hydrophilic monomer blended with carboxylated multiwalled carbon nanotubes". *Applied Surface Science*, 396, 1478-1489, 2017.
[40] Kaya A, Onac C. "The transport of cr(vi) from chrome plating water by polymer inclusion membrane-based carbon nanomaterial". *Pamukkale University Journal of Engineering Sciences*, 24(7), 1348-1354, 2018.
[41] Zhang S, Fu FJ, Chung TS. "Substrate modifications and alcohol treatment on thin film composite membranes for osmotic power". *Chemical Engineering Science*, 87, 40-50, 2013.
[42] Azari S, Zou LD, Cornelissen E. "Assessing the effect of surface modification of polyamide RO membrane by L-DOPA on the short range physiochemical interactions with biopolymer fouling on the membrane". *Colloids and Surfaces B-Biointerfaces*, 120, 222-228, 2014.
[43] Saki S, Uzal N. "Surface coating of polyamide reverse osmosis membranes with zwitterionic 3-(3,4-dihydroxyphenyl)-L-alanine (L-DOPA) for forward osmosis". *Water and Environment Journal*, 34(3), 400-412, 2020.
[44] Jiang JH, Zhu LP, Zhang HT, Zhu BK, Xu YY. "Improved hydrodynamic permeability and antifouling properties of poly(vinylidene fluoride) membranes using polydopamine nanoparticles as additives". *Journal of Membrane Science*, 457, 73-81, 2014.
[45] Cath TY, Elimelech M, McCutcheon JR, McGinnis RL, Achilli A, Anastasio D, Brady AR, Childress AE, Farr IV, Hancock NT, Lampi J, Nghiem LD, Xie M, Yip NY. "Standard methodology for evaluating membrane performance in osmotically driven membrane processes". *Desalination*, 312, 31-38, 2013.
[46] Zhang RX, Braeken L, Luis P, Wang XL, Van der Bruggen B. "Novel binding procedure of TiO_2 nanoparticles to thin film composite membranes via self-polymerized polydopamine". *Journal of Membrane Science*, 437, 179-188, 2013.
[47] Wu HQ, Liu YJ, Mao L, Jiang CH, Ang JM, Lu XH. "Doping polysulfone ultrafiltration membrane with TiO_2-PDA nanohybrid for simultaneous self-cleaning and self-protection". *Journal of Membrane Science*, 532, 20-29, 2017.
[48] Zhang RX, Braeken L, Liu TY, Luis P, Wang XL, Van der Bruggen B. "Remarkable anti-fouling performance of TiO_2-modified TFC membranes with mussel-inspired polydopamine binding". *Applied Sciences-Basel*, 7(1), 1-15, 2017.
[49] Wang Z, Zou Y, Li YW, Cheng YY. "Metal-containing polydopamine nanomaterials: Catalysis, energy, and theranostics". *Small*, 16(18), 1-21, 2020.
[50] Shabani Z, Mohammadi T, Kasiri N, Sahebi S. "Development of high-performance thin-film composite FO membrane by tailoring co-deposition of dopamine and m-phenylenediamine for the caspian seawater desalination". *Desalination*, 527, 1-14, 2022.
[51] Van Wagner EM, Sagle AC, Sharma MM, La YH, Freeman BD. "Surface modification of commercial polyamide desalination membranes using poly(ethylene glycol) diglycidyl ether to enhance membrane fouling resistance". *Journal of Membrane Science*, 367(1-2), 273-287, 2011.
[52] Wang J, Wang YM, Zhu JY, Zhang YT, Liu JD, Van der Bruggen B. "Construction of TiO_2@graphene oxide incorporated antifouling nanofiltration membrane with elevated filtration performance". *Journal of Membrane Science*, 533, 279-288, 2017.
[53] El-Aassar AHMA. "Improvement of reverse osmosis performance of polyamide thin-film composite membranes using TiO_2 nanoparticles". *Desalination and Water Treatment*, 55(11), 2939-2950, 2015.
[54] Kwak SY, Jung SG, Kim SH. "Structure-motion-performance relationship of flux-enhanced reverse osmosis (RO) membranes composed of aromatic polyamide thin films". *Environmental Science & Technology*, 35(21), 4334-4340, 2001.
[55] Lind ML, Ghosh AK, Jawor A, Huang XF, Hou W, Yang Y, Hoek EMV. "Influence of zeolite crystal size on zeolite-polyamide thin film nanocomposite membranes". *Langmuir*, 25(17), 10139-10145, 2009.
[56] Emadzadeh D, Lau WJ, Matsuura T, Rahbari-Sisakht M, Ismail AF. "A novel thin film composite forward osmosis membrane prepared from PSF-TiO_2 nanocomposite substrate for water desalination". *Chemical Engineering Journal*, 237, 70-80, 2014.
[57] Shahrim NA, Abounahia NM, El-Sayed AMA, Saleem H, Zaidi SJ. "An overview on the progress in produced water desalination by membrane-based technology". *Journal of Water Process Engineering*, 51, 1-24, 2023.
[58] Li Y, Li S, Zhang KS. "Influence of hydrophilic carbon dots on polyamide thin film nanocomposite reverse osmosis membranes". *Journal of Membrane Science*, 537, 42-53, 2017.
[59] Azad MJ, Pouranfard AR, Emadzadeh D, Lau WJ, Dil EA. "Simulation of forward osmosis and pressure retarded osmosis membrane performance: effect of TiO_2 nanoparticles loading on the semi-permeable membrane". *Computers & Chemical Engineering*, 160, 1-9, 2022.
[60] Emadzadeh D, Lau WJ, Rahbari-Sisakht M, Ilbeygi H, Rana D, Matsuura T, Ismail AF. "Synthesis, modification and optimization of titanate nanotubes-polyamide thin film nanocomposite (TFN) membrane for forward osmosis (FO) application". *Chemical Engineering Journal*, 281, 243-251, 2015.
[61] Kim CK, Kim JH, Roh IJ, Kim JJ. "The changes of membrane performance with polyamide molecular structure in the reverse osmosis process". *Journal of Membrane Science*, 165(2), 189-199, 2000.

[62] Madsen HT, Hansen TB, Nakao T, Goda S, Sogaard EG. "Combined geothermal heat and pressure retarded osmosis as a new green power system". *Energy Conversion and Management*, 226, 1-10, 2020.
[63] Post JW, Veerman J, Hamelers HVM, Euverink GJW, Metz SJ, Nymeijer K, Buisman CJN. "Salinity-gradient power: Evaluation of pressure-retarded osmosis and reverse electrodialysis". *Journal of Membrane Science*, 288(1-2), 218-230, 2007.
[64] Kim YC, Elimelech M. "Potential of osmotic power generation by pressure retarded osmosis using seawater as feed solution: Analysis and experiments". *Journal of Membrane Scienc*e, 429, 330-337, 2013.
[65] Lin SH, Straub AP, Elimelech M. "Thermodynamic limits of extractable energy by pressure retarded osmosis". *Energy & Environmental Science*, 7(8), 2706-2714, 2014.
[66] Fini MN, Madsen HT, Muff J. "The effect of water matrix, feed concentration and recovery on the rejection of pesticides using NF/RO membranes in water treatment". *Separation and Purification Technology*, 215, 521-527, 2019.
[67] Adhikary S, Islam MS, Touati K, Sultana S, Ramamurthy AS, Rahaman MS. "Increased power density with low salt flux using organic draw solutions for pressure-retarded osmosis at elevated temperatures". *Desalination*, 484, 1-10, 2020.
[68] Jiao Y, Song L, Zhao C, An Y, Lu W, He B, Yang C. "Membrane-based indirect power generation technologies for harvesting salinity gradient energy-a review". *Desalination*, 525, 1-18, 2022.
[69] Abdelkader B, Sharqawy MH. "Temperature effects and entropy generation of pressure retarded osmosis process". *Entropy*, 21(12), 1-14, 2019.
[70] Kokkos N, Sylaios G. "Modeling the buoyancy-driven black sea water outflow into the north aegean sea". *Oceanologia*, 58(2), 103-116, 2016.
[71] Gremes-Cordero S. "The use of thermal satellite data in dense water formation studies in the mediterranean sea". *Journal of Marine Systems*, 20(1-4), 175-186, 1999.
[72] Poulos SE, Drakopoulos PG, Collins MB. "Seasonal variability in sea surface oceanographic conditions in the Aegean Sea (eastern mediterranean): An overview". *Journal of Marine Systems*, 13(1-4), 225-244, 1997.
[73] Çevre, Şehircilik ve İklim Değişikliği Bakanlığı. "Deniz Suyu Sıcaklığı". https://cevreselgostergeler.csb.gov.tr/deniz-suyu-sicakligi-i-85730#_edn1 (18.06.2023).
[74] Touati K, Tadeo F, Hanel C, Schiestel T. "Effect of the operating temperature on hydrodynamics and membrane parameters in pressure retarded osmosis". *Desalination and Water Treatment*, 57(23), 10477-10489, 2016.
[75] Touati K, Tadeo F, Schiestel T. "Impact of temperature on power recovery in osmotic power production by pressure retarded osmosis". *Technologies and Materials for Renewable Energy, Environment and Sustainability (Tmrees14-Eumisd)*, 50, 960-969, 2014.
[76] She QH, Jin X, Tang CYY. "Osmotic power production from salinity gradient resource by pressure retarded osmosis: Effects of operating conditions and reverse solute diffusion". *Journal of Membrane Science*, 401, 262-273, 2012.